IIETA International Information and Engineering Technology Association
Advancing the World of Information and Engineering

Annales de Chimie - Science des Matériaux
Vol.49, No. 1, February, 2025, pp. 71-82
Journal homepage: http://iieta.org/journals/acsm

Preparation and Characterization of Structural and Biological Properties of Nano-Hydroxyapatite Composite Films with Saffron Dye Based on Polymethylmethacrylate

Dhulfiqar Ali Hameed*, Mohammed Hadi Shinen, Abbas Ibrahim Obayes

Department of Physics, Colleges of Science, University of Babylon, Babylon 51002, Iraq

Corresponding Author Email: sci486.zuelfakar.ali@uobabylon.edu.iq

https://doi.org/10.18280/acsm.490110

Received: 20 August 2024
Revised: 19 February 2025
Accepted: 24 February 2025
Available online: 28 February 2025

Keywords:
antibacterial, antifungal, hydroxyapatite, medicine, PMMA, saffron dye, dip-coating, dental fellers

ABSTRACT

This study aimed to prepare and characterize nano-hydroxyapatite, combine it with PMMA, and incorporate saffron dye to enhance the functionality of the composites. A HAP powder was created using fish bone remains and added to PMMA, with saffron dye in varying proportions (0.2, 0.4, 0.6) g. The dip coating method was used to synthesize films and analyze their structural characteristics, while established protocols for microbial cultivation and measuring inhibition zones were followed. It was very small, with a crystalline size of 45-55 nanometers and a width of 20-25 nanometers. After the mixing and compound formation process, the compounds (PMMA\Nano-HAP + saffron dye) were examined by FTIR spectroscopy in third proportions (0.2, 0.4, 0.6) g. Adding 0.6 g of nanoparticles fills all voids in the chloroform-formed polymer, creating a dense crystalline structure with a balanced distribution and agglomeration of HAP, ensuring complete filling for PMMA. The study evaluated the antibacterial efficiency of four bacteria, revealing antifungal activity against Candida albicans. The highest effective inhibition was 15 at 0.6% against Candida albicans. The highest inhibition ratios were 17 for S. aureus, 18 for S. epidermidis, 27 for P. aeruginosa, and 28 for E. coli. The polymer PMMA/Nano-HAP-saffron dye significantly impacts its mechanical properties and exhibits antibacterial and antifungal properties.

1. INTRODUCTION

Composite materials have gradually become more widely used over the past forty years, which has culminated in an extensive array of contemporary medical applications for these substances. The nomenclature "composite" denotes a heterogeneous macroscopic amalgamation of two or more constituents that vary in composition, morphology, and generally physical characteristics to yield specific mechanical, chemical, and physical attributes [1]. In the field of medicine, a biomedical compound is characterized as comprising two or more dispersed active constituents that collectively exhibit properties not represented by any individual constituent when examined in isolation. The uniquely designed attributes are tailored to fulfill a distinct functional requirement as mandated by the specific application of the biomedical compound [2]. Polymethyl methacrylate is a polymer derivatized from the monomer methyl methacrylate (MMA). It is widely used in various applications, including medical implants. Its chemical formula is $CH_2=C(CH_3)COOCH_3$ [3]. The PMMA nanocomposite, which is infused with dye, plays a vital role in drug delivery capsules, colloidal crystals, biomarkers, and nanosensing devices. Its synthesis can be achieved through two methods: the polymerization of MMA (methyl methacrylate) or the formation of covalent bonds, alongside the adsorption of dye molecules onto or within PMMA nanoparticles via physical interactions or chemical bonding [4]. PMMA is the primary polymer in the methacrylate family, synthesized via methyl methacrylate polymerization. This polymer is characterized by low density, exceptional stability, and durability, alongside favorable blood compatibility, biocompatibility, and optical clarity, making it applicable in various biomedical fields, including bone tissue engineering and orthopedic procedures requiring strong, lasting structures [5, 6]. One of the most commonly used polymers, it is frequently combined with nanoparticles to create polymer composites. The addition of nanoparticles into the PMMA matrix is typically performed to improve its performance and functionality [7]. The revival of nanostructured materials is due to their lower dimensionality. These materials, originating from nanoparticles, improve functional properties via synergistic interactions. Numerous biological applications, including drug delivery, biosensing, biocatalysis, and theranostics, depend critically on nanoscale dimensions [8, 9]. Nanostructured Materials Based on Noble Metals for Enhanced Biological Applications. Due to its non-toxic and non-inflammatory properties, as well as its biocompatibility and bioactivity, hydroxyapatite (HAP) is one of the most widely used gold-standard materials and can thus be applied in clinical settings [9]. Because of its biocompatibility, hydroxyapatite is a good choice for biomaterial applications [10]. Human and animal bones are made up of hydroxyapatite [11]. The main component of the mineral bone is hydroxyapatit (Ca10(PO4)6(OH)2) (HA) Molecular structure

of hydroxyapatite (Waste containing hydroxyapatite is occasionally found in natural sources. One technique for creating hydroxyapatite is the calcination process. The hydroxyapatite is calcined and sintered to achieve the required Ca/P ratio [12]. Given that Hydroxyapatite (HAP) constitutes the predominant inorganic mineral constituent of human osseous tissue, calcium phosphate-derived biomaterials have garnered significant scholarly interest [13]. Using a heat treatment technique, fish bones were transformed into HAP at various temperatures and conversion times [14].

Research on polymers and dyes together is one of the most promising areas in functional macromolecules. As a result, colored polymers are playing a bigger role as materials for various technical applications. These days, dye-containing polymers are frequently used in medical applications. Given that the nature of the dye, which is integrated into the polymers, is clearly related to these applications [15]. Saffron has been employed as a coloring agent, as a therapeutic substance, and additionally as a component in cosmetics and perfumery. Nonetheless, there exists evidence of growing interest in this natural pigment due to its diverse array of potentially advantageous functional attributes [16]. The pharmacological benefits of saffron include antispasmodic, expectorant, stomachache relief, and antibacterial properties. Safranal and crocin compounds have been identified as the cause of the antimicrobial properties of saffron extracts [17]. These substances contribute to microbial death by being volatile and/or water soluble, which makes it easy for them to reach the contaminant microorganism [18]. The significance of chromatic polymers as substances for a multitude of technical applications has increased consequently [19]. Saffron and its derivatives have been used in traditional medicine for their various therapeutic effects, including sedative, analgesic, antiemetic, antispasmodic, and antidepressant properties. Additionally, saffron is utilized as a hypnotic and anticonvulsant agent. Research has explored saffron's potential to treat irregular menstruation, with traditional beliefs suggesting that it may function as an emmenagogue to stimulate menstruation in cases of amenorrhea. Furthermore, saffron can help alleviate spasmodic symptoms and may induce miscarriage or abortion. Its stimulating properties may also enhance mental health. In Ayurvedic medicine, saffron is regarded as an adaptogen that aids individuals in coping with stressors such as anxiety, fatigue, and trauma. This article proposes the use of natural saffron dye combined with nano-hydroxyapatite (nano-HAP) as a filler in PMMA composites to enhance their biomechanical and biological properties, leveraging the antioxidant and anti-inflammatory effects of saffron dye to improve wound healing and reduce the risk of infections associated with implants, ultimately aiming to contribute to the development of a new generation of highly efficient orthopedic implant materials [20]. This article proposes the use of natural saffron dye combined with nano-hydroxyapatite (nano-HAP) as a filler in PMMA composites to enhance their biomechanical and biological properties, leveraging the antioxidant and anti-inflammatory effects of saffron dye to improve wound healing and reduce the risk of infections associated with implants, ultimately aiming to contribute to the development of a new generation of highly efficient orthopedic implant materials. This study encompasses the formulation and examination of nano-hydroxyapatite (nano-HAP) alongside the development of an innovative polymethyl methacrylate (PMMA)-based polymer composite through the integration of a natural saffron dye with the nanomaterial synthesized via a stacking methodology, which includes the surface modification of HAP nanocrystals utilizing the natural dye derived from Crocus sativus to augment their organic affinity and compatibility within the PMMA matrix.

2. MATERIALS AND METHODS

2.1 Materials

Poly (methyl methacrylate) is used in granular form. Provenance of poly (methyl methacrylate) is Shanghai Kaidu Industrial development Co, Ltd, China, saffron dye extraction Through Dehydration: Crocus was extracted using According to the method used in the source [19], Chloroform (IUPAC name, trichloromethane) has the formula $CHCl_3$, and it is Organic Solvent, clear, colorless, strong-smelling, and dense liquid.

2.2 Preparation of hydroxyapatite (HAP)

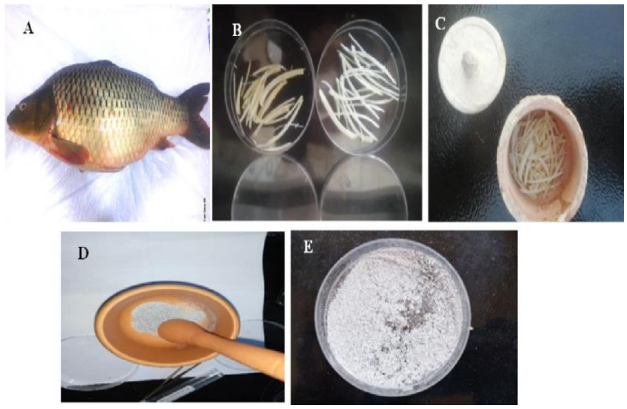

Figure 1. Formation of Nano-HAP utilizing the calcination process

In living organisms, hydroxyapatite (HAP) can be found in nature. Some widely reported sources for the extraction of natural HAP include fish bones and scales, marine coral, and eggshells from marine and bovine sources. Among these options, fish bones are considered the best medium for the extraction of natural hydroxyapatite. Additionally, acquiring fish bones for HAP extraction can be a cost-effective source. Herein, Carp fish purchased from commercial stores were utilized in the synthesis of HAP. The carp is a common term for several freshwater fishes of the carp family, a very large group of fishes originating from Eurasia and Southeast Asia. All carp are sometimes considered by some to be carp, and the carp family itself is often commonly known as the carp family. Figure 1(A) shows an image of carp fish used in the current research. Firstly, the fish was well cocking in a home furnace with fixing temperature about 220℃ for 60 minutes. After naturally cooling to (0℃), the bones of this cooked fish were extracted boiling with diastral water for two hours with quite fire for 30 mints. Finally, the boiled bones were cleaned using ethanol to ensure that all suspension meat and impurities were removed. The final fish bones were kept in a clean peltry dish, as shown in Figure 1(B). The cleaned fish bones were put in a homemade ceramic crucible, as shown in Figure 1(C). An oxy-acetylene flame was applied directly under the tight ceramic crucible, where the temperature reached about 1000℃. The

fish bones will convert into a grayish powder after 20 minutes. To get a final fine sample, the powder was grinding using a mortar as shown in Figure 1(D, E), and then put this powder in a clean test tube to keep it clean and away from the impurities which now ready to investigations the characterizations such XRD, FTIR, FESEM as shown in Figure 2.

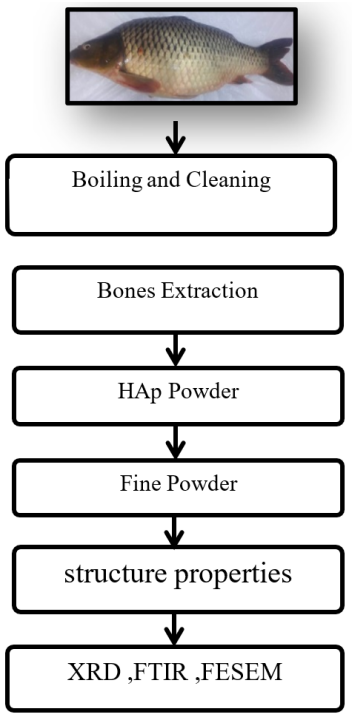

Figure 2. Block diagram of the experimental steps. of Nano-HAP

2.3 Preparation of (PMMA/ HAP+ Crocus sativus l.) Nano composites

Two grams of (PMMA) was dissolved fully in 63 ml chloroform in a glass beaker for Thirty minutes under continual stirring with temperature 25℃. Then, when the pure sample has been dissolved, the amount of HAP is added in different ratios (0.2, 0.4 and 0.6) g, and then a glass beaker into ultra-sonic device to disperse of nanomaterial's for 5 min, As shown Table 1. The dye was added to 10 ml for the mixture and each ratio added 100% (PMMA-HAP) and diverse samples have been formed. The slides were secured with a custom-made clamp and dipped for 10 minutes by using Dip-coating techniques. The slides were simultaneously lowered and retracted at a speed of 240 mm/min. The duration of inactivity was recorded as 10 seconds at both the bottom and the surface. After this, the coated slides were placed on the dip coater for 30 minutes to allow for the evaporation of chloroform and the sedimentation of nanoparticles on the surface.

Table 1. Weight percentages of (PMMA/ HAP+ Crocus sativus l.) Nanocomposites

PMMA g	Nano-HAP g
2	**0**
1.8	0.2
1.6	0.4
1.4	0.6

2.4 Testing of the antibacterial (PMMA/ HAP+ Crocus sativus l.) nanocomposites

A survey was performed to investigate the biologic influences of PMMA/Nano-HAP+ saffron dye nanocomposite on the various species of bacteria, either positively or negatively, that were sourced from multiple hospitals in Iraq. The antimicrobial characteristics of the Nanocomposite (PMMA/Nano-HAP+ saffron dye) were assessed through a susceptibility test, which focused on two types of bacteria commonly present on the human skin. The agar well dispersion technique was employed to estimate the antibacterial activities of the bioactive (PMMA/ HAP+ Crocus sativus l.) against the above-mentioned bacteria. By utilizing cork borers with a 6mm diameter, wells were established. Mueller-Hinton Agar was utilized as the negative control, while various antibiotics were employed as positive controls, depending on the specific pathogenic bacteria under examination. All bacterial isolates utilized in this study were collected from hospitals located in the city of Hillah, Iraq (Table 2).

Table 2. Species and their source of bacterial organisms

No.	Bacteria Isolate	Type of Bacteria as Gram	Type of Specimen
1	**Staphylococcus aureus**	**positive**	**Burns**
2	Staphylococcus epidermis	positive	skin infections
3	**Pseudomonas**	**negative**	**Burns**
4	Escherichia coli	negative	skin infections

2.5 Testing of the antimicrobial (PMMA/ HAP+ Crocus sativus l.) nanocomposites

A research investigation was conducted to analyze the antifungal special effects of a nanocomposite (PMMA/Nano-HAP + saffron dye) on mycosis caused by Candida albicans, specifically focusing on the strain typically found on human skin. Specimens were obtained from the Mycoses Laboratory at the University of Babylon, College of Science. The study employed the agar disc diffusion method, using Potato Dextrose Agar as a negative control and a fungal strain as a positive control to determine the antifungal efficacy of the nanocomposite. Cotton swabs were used to prepare the Petri dishes. A 50 µl suspension of 0.5 C. albicans was inoculated onto the agar. Afterward, the nanocomposite disk samples, previously cultured with the fungi, were placed on the agar medium. The agar plates were then incubated for 48 hours at a controlled temperature. The antifungal properties of the nanocomposite, presented in tablet form, were evaluated through a susceptibility testing procedure. Specifically, the agar-well diffusion technique was implemented to assess the effectiveness of the nanocomposite against Candida albicans-induced mycosis. The sizes of the areas were measured. The damping formed around the samples using a digital caliper three times. cork porers with a diameter of 6 mm, wells were created. Potato dextrose agar was employed as the negative control, and mycoses were used as the positive control.

2.6 Dip coating

The dip coating method is recognized as an easily accessible

and frequently utilized technique for the fabrication of thin films using a diverse array of inorganic, hybrid, and nanocomposite materials [20]. The dip-coating process is demonstrated in Figure 3. It allows for the coating of a wide variety of substrates and complex geometries, such as substrates containing holes or intricate patterns, enabling a high level of control over important parameters and providing a degree of flexibility that is unattainable with conventional methods. Essentially, the substrate intended for coating is immersed in the initial solution and then removed at a consistent speed during the process, which is conducted under carefully controlled temperature and air conditions. Precise regulation of the withdrawal rate and evaporation conditions enables fine adjustment of film properties, including thickness, optical characteristics, and internal structure. The solution spreads uniformly across the substrate's surface due to the combined effects of viscous drag and capillary action. Film gelation occurs during the final stages of the process as evaporation occurs. Substrates that have been coated often undergo post-heat treatment, which can impact the film's properties [21].

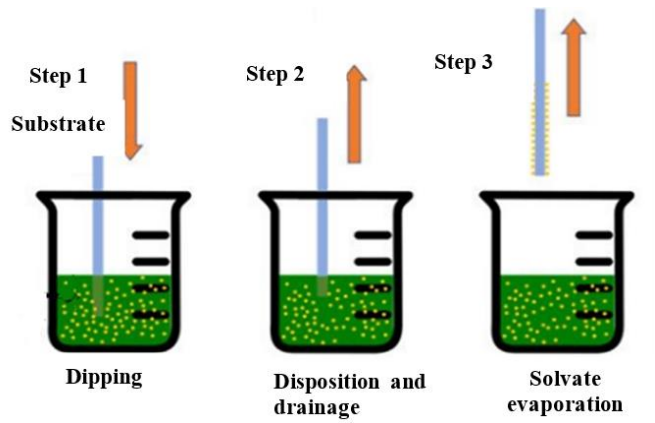

Figure 3. The phases of the dip-coating technique for thin-film deposition in order of succession: Step 1: The mixture is dipped and submerged into the substrate. Stage 2: A constant rate of substrate withdrawal. Stage 3: The thin film is created by solvent evaporation [22]

3. CHARACTERIZATIONS STRUCTURALLY: OUTCOMES

3.1 XRD diffraction analysis

Hydroxyapatite has historically been considered a strong candidate due to its bioceramic characteristics, attributed to its resemblance to the mineral composition found in bone structure. Its capacity for promoting bone growth through osteoconductive properties and its compatibility with living tissues further enhance its utility in bone grafting procedures [23].

Hence, this study was to produce nano-HAP without any additional chemicals. The phases and purity of the derived HAP crystals (synthesized from natural and artificial sources) were verified by XRD analysis. The XRD patterns of HAP particles manufactured from fish Bone are illustrated in Figure 4. The crystal phase analysis of HAP powder from the bio-source was carried out by X-ray diffraction (XRD) investigations. The phases were defined by comparing the experimental XRD pattern with the standards complied by the International Center for Diffraction Data (ICDD) using tags 00-009-0432 for the hexagonal Hydroxyapatite structure. Every Hydroxyapatite pattern was revealed as a single phase. A well-resolved, well-defined characteristic peak with the highest intensity of HAP was obtained at a 2θ value of 31.77°, corresponding to plane 211. The formed phase was pure and well-matched to the standard pattern. The standard plane corresponding to the HAP plane (i.e., 002, 210, 210, 211, 112, 211, 211, 202, 222, 213, 004) was well observed, which proved the purity of the HAP crystal line powder [24, 25]. Sharp peak intensity and well-resolved peaks in XRD patterns of the powders at high calcination temperature proves complete crystallization of the powder.

The crystal sizes of HAP were estimated with Scherrer's equation $D = 0.9\,\lambda / B \cos\theta$. where D is the average grain size, B is the full width at half-maximum peak, λ is the diffraction wavelength (0.154059 nm), and θ is the diffraction angle. The Bragg reflection at (211) levels of HAP was investigated to calculate the crystal size. The crystal size of HAP synthesized from fish bones & cattle bones is 17.24 nm.

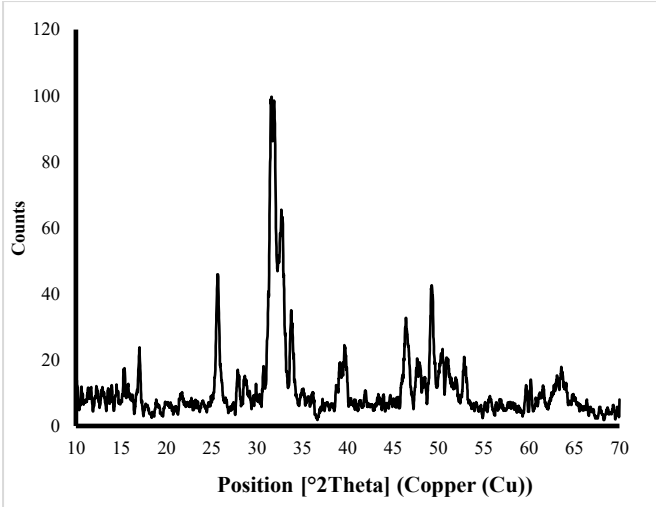

Figure 4. FESEM illustrates of Nano-hydroxyapatite(Nano-HAP)

3.2 FESEM analysis for the nano-hydroxyapatite (Nano-Hap)

Field emission Scanning electron Microscopy (FE-SEM) facilitates the acquisition of more distinct images with reduced electrostatic distortion and a spatial resolution reaching as low as 1.5 nm. Its performance surpasses that of conventional SEM by a factor of three to six. The investigation of the surface morphology and crystal dimensions of hydroxyapatite derived from raw fish bone was conducted using FESEM. The FESEM image in Figure 5 depicts the hydroxyapatite obtained from raw fish bone at a temperature of 1000°C. The microcrystals of hydroxyapatite within the natural fishbone exhibit small dimensions, with a crystalline size ranging from 45 to 55 nm, a width of 20-25 nm, and lengths exceeding a few micrometers. The nanostructures observed in raw fish bone are notably compact due to the presence of organic components. The formation of these microstructures in the hydroxyapatite heat treatment process is the result of the inclination of the particulate matter to coalesce and crystallize at higher and higher temperatures. The resulting powder from heat treatment at specific temperatures is characterized by clearly defined, randomly oriented structures resembling spheres. In certain

regions, the presence of some clusters of doped HAP nanoparticles suggests nanoparticle agglomeration. This structure presents a combination of nano- and microstructural configurations, as depicted in the accompanying Figure 5.

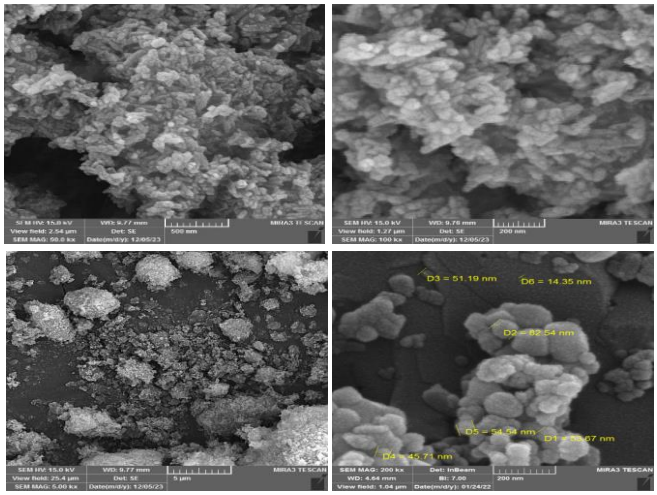

Figure 5. FESEM illustration of nano-hydroxyapatite (Nano-HAP)

3.3 ATR-FTIR spectroscopy for the composites (PMMA\Nano-HAP + Saffran dye)

The interpretation of peaks in an infrared (IR) spectrum depends on the vibrational modes of the molecular bonds present in the sample. Given the composite nature of your sample (PMMA, hydroxyapatite, and saffron dye). To observe the hierarchical effects of nano-HAP with the incorporation of saffron dye on the PMMA matrix, FTIR was carried out. The FTIR is displayed in Figure 6. The molecular structure is analyzed to determine the phase content, which includes the amount of nano-hydroxyapatite and saffron dye added to the polymer, which forms the foundation of the composite. was performed using FTIR. The presented data accounts for six independent samples and surveys. Samples were scanned from about 500 to 4000 cm-1 with a resolution of 2 cm^{-1} and a total of 32 scans.

The FTIR spectra of unmodified PMMA particles and PMMA particles modified by a ratio of Nano-HAP and saffron dye are displayed (550–4000 cm^{-1}). Every group's spectrum was comparable and displayed the distinctive absorption peaks of PMMA. In the infrared (IR) spectrum of poly (methyl methacrylate) (PMMA), peaks at various wavenumbers correspond to different vibrational modes within the molecule. The peaks at 1485.22 cm^{-1} are related to the stretching of the C-H bonds in the methyl. 1737.86 cm^{-1} and 1731.82 cm^{-1}. These are usually related to the stretching of the C=O bonds in the carbonyl group and are characteristic of the ester groups in PMMA. 2844.61 cm^{-1} and 2994.66 cm^{-1}: These peaks indicate the stretching of the C-H bonds in methylene and methyl. The peak 3435.68 cm^{-1}: May be related to O-H bond stretching, which could be due to the presence of impurities [25, 26].

The FT-IR spectra of bony fish (Nano-HAP), shells, and calcined shells heated to 1000°C demonstrated distinct characteristic peaks of hydroxyapatite (HAP). A notable number of bands were identified in the spectra, specifically at 565, 603, 876, 962, 1035, 1412, 1421, 1458, 1637, 2855, and 2927 cm^{-1}, as well as a band observed in the range of 3000-3800 cm^{-1}. These bands closely match those found in reference spectra for HAP. Additionally, bands corresponding to the phosphate (PO_4) group were observed at 565, 603, 876, and 962 cm^{-1}. This may be due to the removal of all the organic material from the raw (fishbone) and formation of HAP crystals. Thermal stability is an important feature of derived HAP. Additionally, the FTIR spectra sample exhibited a peak at 632 cm^{-1} and a broad peak at 3300– 3800 cm^{-1} due to the presence of the hydroxyl group. The intense peaks observed at 1412 and 1458 cm^{-1} in the spectrum of calcined fishbone are attributed to CO_3. according to prior investigations [27, 28].

The interpretation of peaks in the infrared (IR) spectrum of saffron dye involves understanding the vibrational modes of its constituent functional groups. 582.28 cm^{-1}. This peak could correspond to bending vibrations of aromatic C-H bonds. These vibrations are common in aromatic compounds. 1073.77 cm^{-1}. This peak may correspond to C-O stretching vibrations, indicating the presence of carbonyl groups (C=O) or ether linkages (C-O-C) within the saffron dye molecule. 1647.27 cm^{-1}. This peak might represent the stretching vibration of C=C bonds, which are characteristic of aromatic rings present in saffron dye. 2984 cm^{-1}. This peak likely corresponds to stretching vibrations of C-H bonds. It may arise from various types of C-H bonds present in the saffron dye molecule, such as methyl (CH3) or methylene (CH2) groups [28, 29].

The FTIR spectrum of PMMA, when combined with nano-hydroxyapatite (0.2g) and saffron dye, reveals several peaks, including O-H stretching vibrations, C-H stretching vibrations, C≡C stretching vibrations, C≡C stretching vibrations, C=O stretching vibrations, C=O stretching vibrations, N-H bending vibrations, and C=C stretching vibrations. These peaks provide insights into the functional groups and interactions present in the modified PMMA, which may be due to moisture or surface hydroxyl groups on the nano-hydroxyapatite. The peaks also correspond to C≡C stretching vibrations, alkyne groups, triple bond interactions, C=O stretching vibrations, ester groups, and N-H bending vibrations. These findings offer valuable insights into the functional groups and interactions in PMMA [30-32].

When adding 0.4 g of nano-hydroxyapatite with 10 ml of saffron dye to PMMA, the FTIR spectrum shows the peaks(3909.83 cm^{-1}, 3890.68 cm^{-1}, 3843.71 cm^{-1}, 3826.05 cm^{-1}, 3807.81 cm^{-1}, 3716.69 cm^{-1}, 3695.59 cm^{-1}, 3680.81 cm^{-1}, 3659.97 cm^{-1})These peaks are likely associated with the stretching vibrations of hydroxyl (O-H) groups, which can be present due to moisture or surface hydroxyl groups on the nano-hydroxyapatite(1,2). 3787.58 cm^{-1}. This peak also corresponds to O-H stretching vibrations, indicating the presence of hydroxyl groups1. 3572.32 cm^{-1}. This peak is related to the stretching vibrations of O-H groups hydroxyl groups1. 3434.86 cm^{-1}. This peak is typically associated with O-H stretching vibrations, possibly from hydroxyl groups1. 2929.45 cm^{-1}: This peak is indicative of C-H stretching vibrations, which are common in organic compounds such as PMMA2. (2366.34 cm^{-1}, 2345.57 cm^{-1}) These peaks might be associated with C≡C stretching vibrations, indicating the presence of alkyne groups2. (1736.15 cm^{-1}) This peak is typically associated with C=O stretching vibrations, common in ester groups present in PMMA2. (1552.76 cm^{-1}) This peak could correspond to N-H bending vibrations or C=C stretching vibrations in aromatic rings [30, 31, 33].

When adding 0.6 g of nano-hydroxyapatite with 10 ml of saffron dye to PMMA, the FTIR spectrum shows the peaks that the interpretation of the peaks: (3650.98 cm^{-1}) these are

associated with O-H stretching vibrations, indicating the presence of hydroxyl groups. (3435.12 cm^{-1}) Also associated with O-H stretching vibrations, possibly from absorbed water or hydroxyl groups. (2992.69 cm^{-1} and 2929.51 cm^{-1}) Indicative of C-H stretching vibrations, which are common in organic compounds such as PMMA. (1735.64 cm^{-1}) Typically associated with C=O stretching vibrations, common in ester groups present in PMMA. (1686.28 cm^{-1}, 1654.91 cm^{-1}). These peaks correspond to C=C stretching vibrations, indicating the presence of aromatic rings in the composites [26, 32, 33].

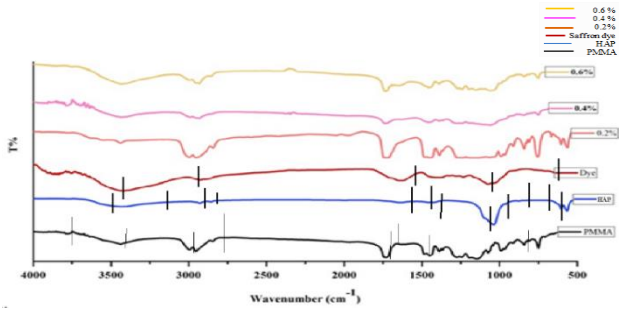

Figure 6. FTIR spectroscopy illustration of composites (PMMA\Nano-HAP+saffran dye)

3.4 Analyzing morphology by SEM (Scanning Electron Microscope)

The SEM evaluation examines the structure and morphology of PMMA and PMMA/nano-AP+ saffron dye regardless of the applicable variables. The scanning electron microscopy (SEM) of pure PMMA\Nano-HAP + saffran dye Nanocomposites is illustrated in Figure 7, prepared by the dipping method with different magnifications.

FESEM was used to monitor the dispersion and distribution of HAP nanoparticles within the PMMA polymer base. Figure 7 (A1) to (A4) shows SEM images of the pure polymer at different magnification powers (2 µm), (500 nm), and (200 nm).

Figure 6 shows an FESEM image of the pure PMMA formed by the dip coating method. Figure 7 (A1) FESEM of PMMA at magnification (2um), which shows the polymer granules formed evenly on the surface. Figure 7 (A2) shows the pure polymer under magnification power (500nm). We notice that the surface of the polymer contains pits or small circular gaps of varying sizes distributed on the surface of the polymer, and this is confirmed by the image at magnification power (200nm). This is the result of the organic solvent, which is chloroform, resulting from the diving process [34].

Figure 7 (B1) illustrates an image of SEM of the composite formed from the PMMA by adding (0.2 g) of nano-HAP with saffron dye by the dip coating method. Figure 7(B1) illustrates the image of FESEM of the composite formed at a magnification power of (2 mu), where we notice that the surface formed contains small pits and gaps compared to the pure PMMA. Figure 7 (B2, B3) appears for the composite formed at a magnification power of (500nm). We notice that the surface of the compound is clear and is coated with nanomaterial and dye. In addition to that, it contains gaps at a magnification power of (200nm). We notice that the surface of the composite formed is completely coated with the Nano-HAP and the dye. This is the result of the agglomeration of the nanoparticles and saffron dye particles on the surface of the PMMA. We can see the pits and cavities that were not covered by the Nano-HAP and the dye, as their distribution is uneven. This results in the agglomeration of the Nano-HAP and saffran dye very quickly in the chloroform, which permeates the surface PMMA during the diving process. When (0.2 g) of Nano-HAP and saffran dye were added, irregularly sized holes were formed on the PMMA interface, and the Nano-HAP and saffran dye did not spread in a uniform and homogeneous manner. High-magnification SEM showed that most of the Nano-HAP and saffran dye had filled the pits on the surface, but they were not enough, and this indicates. However, the concentration of Nano-HAP (0.2 g) was not sufficient to completely fill the holes in the PMMA [34-36]. Figure 7(C) shows a SEM of the composite formed from the polymer when adding (0.6g) of Nano-HAP with saffron dye by the solvent immersion method. Figure 7 (C1) is the SEM of the composite formed at a magnification power of (2 mu), where we notice that the Nano-HAP and the saffron dye It is spread over the surface and have sharp edges without gaps compared to the pure PMMA. The percentage (0.6g) appears for the composited formed at a magnification of (500nm). We notice that the surface of the composite is clear and is coated with Nano-HAP and saffran dye, which can be observed. At a magnification power of (200nm) in Figure 7 (C4), we noticed that the PMMA was completely covered by Nano-HAP, which formed a rough surface and was completely randomly distributed over the entire surface. This indicates that the proportion of the PMMA compared to the Nano-HAP has decreased the tendency. The Nano-HAP agglomerate in solution, which provides sufficient time to place the dispersed Nano-HAP arranged the surface in a more uniform than homogeneous mode [34, 36, 37].

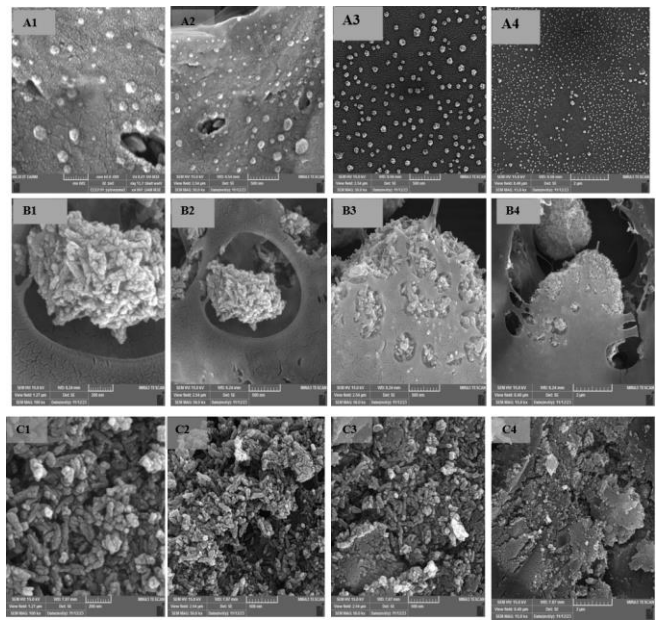

Figure 7. SEM images of Poly (methyl methacrylate) cross-section of unmodified (PMMA pure) (A1–A4), modified PMMA(B1-B4) (PMMA\Nano-HAP (0.2g) +saffran dye) and modified PMMA(C1-C4) (PMMA\Nano-HAP (0.6g) +saffran dye)

3.5 Distributions the nano-HAP in polymer analysis by image J

SEM analysis shows PMMA and PMMA\Nano-HAP +

saffran dye morphology regardless of parameters. Scanning electron microscopy displays pure PMMA\Nano-HAP + saffran dye Nano composite in Figure 8 with various magnifications [38]. The distribution of nanomaterials within a polymer is crucial for composite formation, optimization, and application. SEM is often utilized for sizing nanoparticles. The ruler tool in image analysis software is commonly used to measure nanomaterial diffusion within composites. This method is effective and standard for nanoparticle size distribution analysis [39]. Basically, Image J software is used to analyze the size of a typical nano-HAP in an SEM image and we use Origin software to process the data to get its precise distribution quickly.

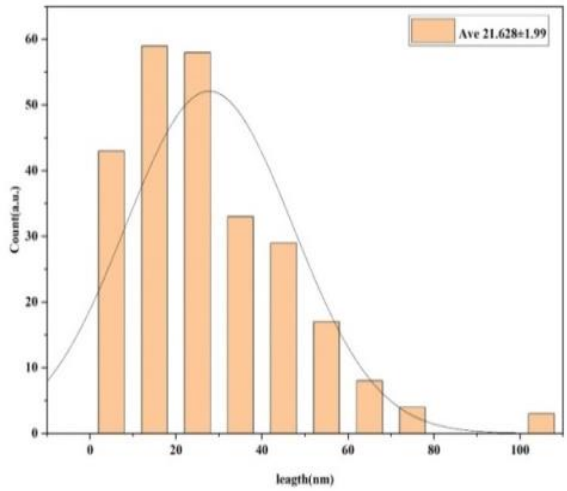

(A)

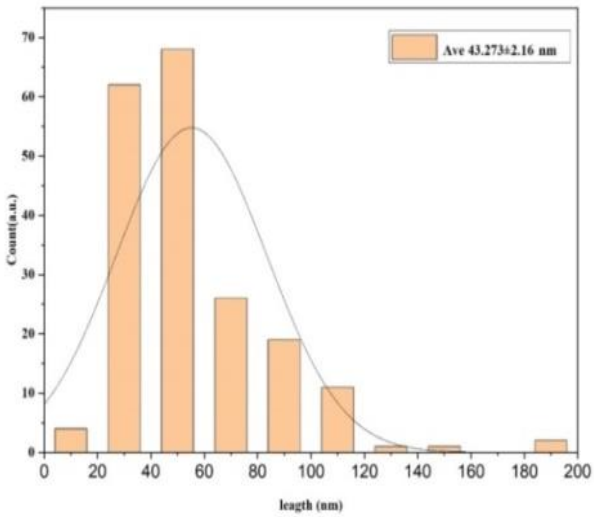

(B)

Figure 8. Illustrated the Distributions of the nano-HAP in PMMA A: modified PMMA (PMMA\Nano-HAP (0.2g) + saffran dye) B: modified PMMA (PMMA\Nano-HAP (0.6g) + saffran dye)

This investigation produced positive findings, as the average size of the Nan-HAP inside the PMMA ranged between (43.273±2.16 nm) at the percentage of (0.2 g), as shown in Figure 7(A). Still, when a percentage of (0.6 g) was added, the average size of the Nan-HAP inside the PMMA ranged between (21.628±1.99), as shown in Figure 8 (B), which indicates the percentage of the material. The greater the percentage of nanoparticles, the more they spread throughout the PMMA and fill the spots inside the polymer surface. Therefore, the combinability is greater, and this is what was proven by SEM images. Loading nanoparticles greatly affects the compound formed's shape, size, and roughness [37, 40]. This indicates that the dimensional distribution of Hydroxyapatite (HAP) has a more uniform profile and shows a tendency toward agglomeration. Additionally, the concentration of Nano-HAP (0.6 g) was sufficient to completely fill the voids [41]. Therefore, the more Nano-HAP, the better the composite, and therefore, the stronger and more durable the composite that was formed. The pits and gaps on the surface of the formed composite no longer existed, and thus, the immersion time was appropriate for the formation of the composite. The addition of the Nano-HAP led to an increase in the agglomeration of the nanoparticles due to the pressure on the growth of the particles. Based on the SEM images, it is difficult to distinguish between Nano-HAP and dye particles because the dye particles are much smaller than nanoparticles [42].

3.6 Effect of the addition of Nano-HAP on hardness of the dental fellers

A hardness refers to the ability of a surface to resist scratching, cutting, and penetration. The filling material is fabricated using a polymer known as PMMA (polymethyl methacrylate). This polymer is soluble in chloroform, an organic solvent represented by the chemical formula $CHCl_3$, which appears as a colorless and highly volatile liquid. Chloroform also serves as an excellent solvent for a variety of chemical compounds, with a density of 1.49 g/cm³. To prepare the material, PMMA is dissolved in 30 ml of chloroform with continuous agitation for 30 minutes. Once the dissolution process is complete, Nano-HAP (hydroxyapatite nanoparticles) is added in specified proportions (0.2, 0.4, and 0.6 grams), along with saffron dye. A magnetic stirrer is then used to mix the polymer and nanoparticles for 10 minutes, achieving a more homogeneous solution at room temperature. The casting technique is employed to fabricate samples of the nanocomposite (PMMA/Nano-HAP + saffron dye) within molds made of stainless steel. These molds are configured as cylindrical cavities with a diameter of 6 mm and a thickness of 10 mm. An iron rod with a diameter of 6 mm and a thickness of 8 mm is inserted into the cavity to create samples with a final thickness of 2 mm. This methodology is used for preparing samples intended for hardness assessment [43]. As shown in Figure 9.

Figure 9. Molds utilized to generate special hardness analysis sample preparations

Table 2 and Figure 10 illustrate that the hardness values increase with the increase in the duration of exposure to light periods because the number of monomers that are converted into polymers will increase, causing an extension of the hardness values of dental fillings [44]. There is also a variation

in the hardness values with the increase in the percentage of Nano-HAP apatite, resulting in increasing load due to the continuous shrinkage of the fillings through the initial spaces, which is associated with incomplete hardening or bonding of the filling. Therefore, hardness values escalate with the rise in the percentage of the HAP.

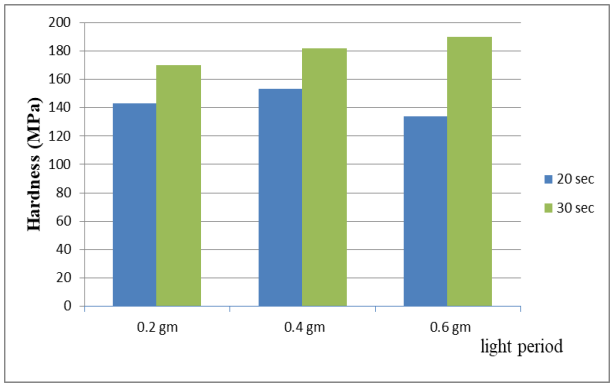

Figure 10. The effect of adding nano-HAP on the hardness property in units (MPa) of the filling over periods of (20 and 30) seconds

3.7 The efficiency of the antibacterial (PMMA/ Nano-HAP+ Crocus sativus l.) nanocomposites

Figure 11 shows the effect of the (PMMA/ HAP+ crocus sativus l). Nanocomposites in samples (0.2, 0.6) on four types of bacteria (Staphylococcus aureus, Staphylococcus epidermis, Pseudomonas, Escherichia coli). It was found that the small percentage of saffron dye and Nano-HAP in the Nanocomposites prevents the growth of positive and negative bacteria. The antibacterial behavior is achieved due to the small amount of nanoparticles and the antibacterial saffron dye, as well as the saffron dye on the surface of the composites. It destroys the cell membranes of bacteria through oxidation and ultimately causes inactivation and inhibition of bacteria.

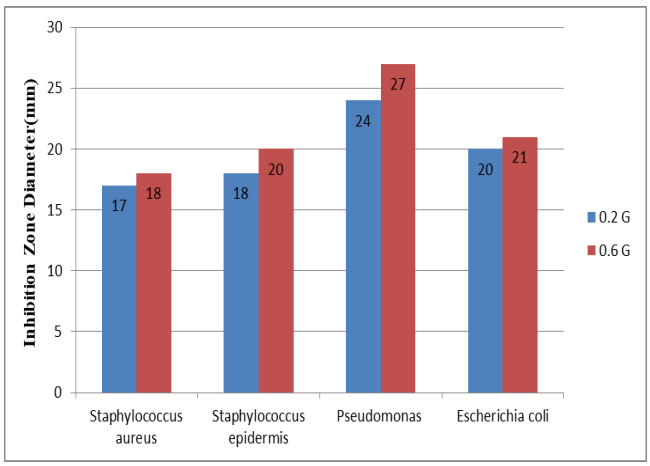

Figure 11. The antibacterial activity of composites of Nanocomposite (PMMA/Nano-HAP+ saffron dye) (0.2, 0.4, and 0.6 ratios) against (Staphylococcus aureus, Staphylococcus epidermis, Pseudomonas, Escherichia coli)

3.8 The efficiency of anti-mycoses activity of nanocomposite (PMMA/Nano-HAP+saffron dye)

Research to determine the antifungal influences of nanocomposites carried out (PMMA/Nano-HAP + saffron dye) on Candida albicans fungi obtained from the Mycology Laboratory / University of Babylon / College of Science. Figure 12 shows a picture of the Petri dish poured into it after pouring PDA into it, while Figure 12 shows a picture of the dish after the process of transplanting colonies of Candida albicans fungi into it. Figure 13 shows the effect of composite samples with different percentages of nanomaterials on the C. albicans fungi. As noted in Figure 13, the percentage of Nano-HAP incorporated into the dye and PMMA affects the inhibition of fungi. This effect is due to the nanoparticles and also to the presence of saffron dye, which contains biologically active terpenoids [45].

Contained within the composites. There are several mechanisms used by this plant dye to conquer the advance of C. albicans, these disruptions affect cell membrane function, energy activity, and fungal cytoplasmic membrane integrity [46]. From the data provided, it can be seen that the composite samples (PMMA/Nano-HAP+ saffron dye) showed significant antifungal effects.

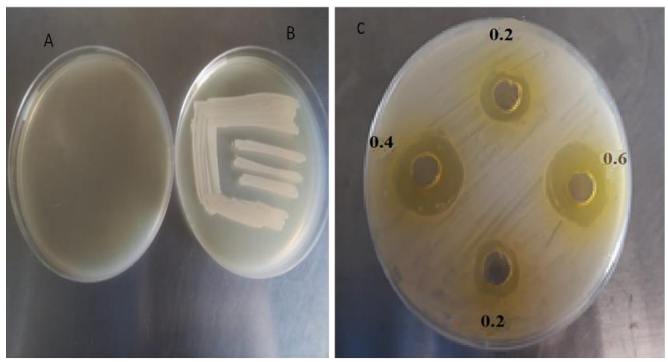

Figure 12. Antifungal inhibition zone of (PMMA\Nano-HAP + saffran dye) (0.2, 0.4, and 0.6 ratios) against C. albicans

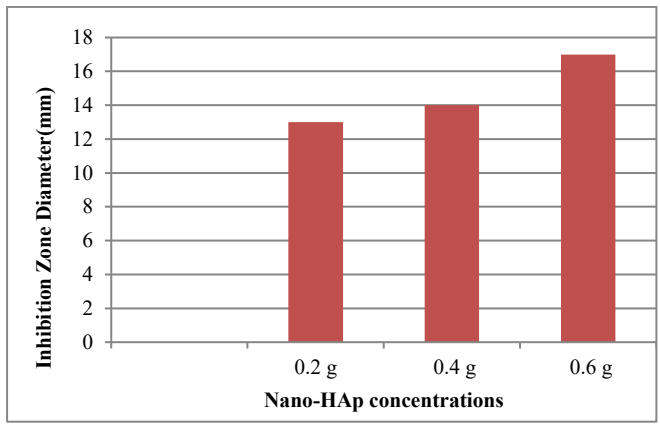

Figure 13. Antifungal inhibition zone of (PMMA\Nano-HAP + saffran dye) (0.2, 0.4, and 0.6 ratios) against C. albicans

4. DISCUSSION

Poly (methyl methacrylate) (PMMA) was the most widely applied in the clinical medical field for its remarkable physicochemical features and compatibility with cells [26]. Using MMA monomer and a free radical initiator, PMMA, a commonly used polymer, is frequently mixed with nanoparticles to create polymer composites that improve their functionality and performance [7]. A biomedical composite is

described as consisting of one or more active ingredients with specially designed general characteristics that none of the constituents in isolation would describe [2].

Hence, this study was to produce Nano-HAP without any additional chemical and mixing with polymer and natural dye. The purity and the phase of the synthesized HAP crystals (from natural and synthetic sources) were confirmed by XRD analysis.

The X-ray patterns of HAP molecules composite from fish bones are shown in Figure 3. Crystal phase analysis of HAP surface powder from the bio-source was performed by X-ray diffraction measurements. The phase generated was pure and matched well with the standard pattern. The crystal size of HAP synthesized from fish bones is 17.24 nm. The hydroxyapatite microcrystals in natural fish bones were very tiny from the FESEM images (4), with crystals 45-55 nm in size, 20-25 nm in width, and more than a few μm in length. The nanostructures of fish bones seemed to be dense due to the presence of organic matter. The formation of these microstructures from hydroxyapatite derivatives in thermal processing may be attributed to the tendency of the particles to crystallize and agglomerate at high temperatures. Recent research has shown that the mechanical characteristics and composition of fish bones, including both osteocytic and anosteocytic varieties, differ. These characteristics set fish bones apart from other vertebrate bone materials and place them in a different class within the bone material [47].

Addressing these issues, in our previous case study, nano-HAP and saffron dye, a versatile cross-linker, were unified into a PMMA-matrix to create the new style of PMMA- and organic-modified PMMA. It was found that when the fraction of nano-HAP does increase, By weight (0.2% 0.4, and 0.6)g, nano-HAP prepared from fish bones and without adding any chemical substance with the saffron dye extracted from the saffron plant into a PMMA provided an antibacterial effect against positive and negative bacteria as well as against the fungi. It was also reported to have a significant beneficial influence on the mechanical characteristics of dental fillings that are associated with increased hardness. From this, it can be concluded that the hardness of the top surface depends on the exposure time, the type of nanomaterial and its percentage in the filler [48]. The increase of the top surface hardness with the increase of the filler ratio is due to the hardness of the filler. Besides, nanomaterial fillers. Nanomaterials rarely have intermolecular spaces; this increases the material's hardness, thus increasing the surface hardness. Each of the investigated nanocomposites demonstrated excellent hardness limitations by ISO (up to 50 MPa). Also, the higher the filler loading, the lower the mechanical properties, namely the hardness property of the top surface and this is in agreement with the source. Fillers, on the other hand, although the fillers are similar in size, include nanoparticles that have unique physicochemical features. These properties are not only a matter of particle size but also relate to the qualities caused by these small-sized particles. They thus have enhanced effects of the fillers they contain making the surface highly resistant to scratching when added [49].

In this study, the compositional properties, antifungal properties, cytocompatibility and other structural and chemical properties were revealed, then the effects specified that the incorporation of nano-HAP and saffron dye into the PMMA polymer significantly affected the activity of Candida albicans, as well as the bacterial activity, without affecting its cellular compatibility. The bioactive and biocompatible properties of HAP make it useful in the biomedical field and it is mostly used in bone tissue regeneration, dental fillings and in the medical field [48]. Saffron dye consists of the dried stigmas of Crocus sativus L., an unusual, matchless and medicinal plant [50]. The antimicrobial activity of saffran is potent owing to the existence of safranal and crocin compounds in their extracts (boyamakale-basl). In traditional medicine, saffron is widely used as a natural healing remedy [50-52]. These characteristics are primarily related to its picrocrocrocin, safranal, and crocin constituents. Picrocrocin is the glycoside precursor of safranal (2,6,6,6-trimethyl-1,3-cyclohexadiene-1-carboxaldehyde), which in turn is the most abundant of the volatile constituents responsible for the odor of this spice. Croconates are the esters of crocetin that contain the sugar compounds glucose, centipoise, Napolitan nose, or tri-glucose [53].

The results of FTIR in Figure 5 demonstrated that all of the groups had the characteristic absorption peaks of PMMA and revealed that the main architectural constituent of all the samples was PMMA. It was also confirmed that new absorption peaks appear in the applied groups when adding Nano-HAP and saffron dye. It is worth noting that some absorption peaks disappeared when adding Nano-HAP at a rate of (0.6 g). This disappearance can be attributed to several factors:

1. Reaction and bond formation: Addition of nano-pigment hydroxyapatite and saffron to PMMA can lead to new reactions and bond formations. These interactions can change the vibration patterns of molecules, causing some peaks to disappear or shift.

2. Effects of concentration: The concentration of added ingredients can affect the intensity and presence of certain peaks. Higher concentrations of nano-hydroxyapatite and saffron dye can lead to stronger interactions, which may mask or eliminate some of the peaks.

3. Physical changes: The physical state of the mixture, such as changes in crystallinity or phase transitions, can also affect the FTIR spectrum [54]. These changes can alter the vibration modes and cause certain peaks to disappear. The enhancement of the structural properties of PMMA modified by Nano-HAP and saffron dye can be observed by studying the results of a SEM, where we notice that the PMMA, through the scanning SEM image, contains pits or small circular gaps varying in size. This is the result of the organic solvent, which is Chloroform resulting from the immersion process during the deposition of membranes using this technique [34]. But when adding the nanomaterial represented by Nano-HAP and saffron dye, the spots and gaps are filled with it and the PMMA tends to agglomerate, and this is confirmed by the electron microscope image when adding (0.6 g). This was also confirmed by analyzing the images using the image program when adding a percentage of (0.6 g) the average size of nanoparticles inside the polymer was between (21.628±1.99), which indicates that the percentage of nanomaterial the higher the percentage, the more it spreads inside the polymer and fills it. The stains are inside the polymer surface, so the compatibility is greater.

Figure 10 shows the composite influence of samples on the sustainability of bacterial strains (S. aureus, Staphylococcus epidermis, Pseudomonas, and Escherichia coli). C. albicans fungi. In Figure 11, it can be understood since the data presented, the composite (PMMA/HAP+saffran dye) showed significant antimicrobial and antifungal effects. The PMMA/Nano-HAP+ saffron dye composite (0.6g) showed

growth inhibition of almost all the microorganisms studied. The results emphasize the decisive contribution of nitrogen to the antimicrobial activity of the considered compounds. This can be attributed to the bacteria-inactivating properties of HA which depend on the adsorption mechanism. It has been proven that penetration of the microbial membrane by composite materials contributes to the disruption of the membrane of its cells as a result of the composite materials [55].

In addition, saffron tincture includes biologically important terpenoids. Also, saffron tincture features crocin (the gentiobiose ester of crocetin), which has biological efficacy. This is mainly due to the abundance of changed classes of phenolic composites in saffron dye [46]. The multiple mechanisms utilized by botanical mines to overpower the advancement of microbial pathogens are several and include disrupting cell membrane function, disrupting activity, and perturbing the cytoplasmic membrane of bacteria [47, 48, 56].

5. CONCLUSIONS

FE-SEM images depicted small aggregates of spherical-shaped particles on the outer surface of PMMA+HAP. The nanocomposites were found to have a spherical shape with grain sizes up to 45.26 nm. The increase in particle size is observed with an increase in the concentration of hydroxyapatite in the PMMA polymer mixed with saffron dye. The study also examined the impact of adding different percentages (2%, 4%, 6%) of these materials on the hardness, as well as their effect on Candida albicans fungi and four types of opportunistic bacteria found on human skin. The study found that increasing the percentage of nanomaterials from 2% to 6% in both powders resulted in higher hardness of the fillers. Tests also confirmed that the effectiveness against fungi and bacteria increased with higher addition rates. Additionally, the tests showed that polymeric composite films containing saffron pigment have antibacterial and antifungal properties.

This study has introduced a novel multifunctional composite material comprising PMMA, nano-HAP, and saffron dye, representing a significant advancement in the field of biomaterials. By leveraging the unique properties of each component, we have successfully developed a composite with exceptional biocompatibility, mechanical strength, and antimicrobial activity. Our findings demonstrate that the super crystalline nano-HAP derived from fish bones, when combined with PMMA and saffron dye, results in a material with a high aspect ratio and well-defined nanostructure. These characteristics, coupled with the inherent antibacterial properties of saffron, make the composite an ideal candidate for various biomedical applications.

Key contributions and potential applications of this research include:

1. Development of a sustainable and cost-effective method for producing high-quality nano-HAP from natural sources.
2. Creation of a multifunctional composite with enhanced mechanical properties and potent antimicrobial activity.
3. Potential for use in dental applications as a durable, antimicrobial dental filling material.
4. Prospects for application in wound care as a sterile film to prevent infections in burns and cuts.
5. Foundation for future research into the development of orthopedic implants and other biomedical devices.

ACKNOWLEDGMENT

The University of Babylon provided crucial measurements and technical assistance, for which the authors are grateful. Additionally, the authors would like to thank Dr. Qasim for carrying out the experimental tests, Dr. Nihad Abdel Amir for helping with the preparation of this paper, and Dr. Safir for looking into the electron microscope image.

REFERENCES

[1] Migliaresi, C., Nicolais, L. (1980). Composite materials for biomedical applications. The International Journal of Artificial Organs, 3(2): 114-118. https://doi.org/10.1177/039139888000300213

[2] Voskerician, G. (2018). Improving the hemocompatibility of biomedical composites. In Hemocompatibility of Biomaterials for Clinical Applications, pp. 357-375. https://doi.org/10.1016/B978-0-08-100497-5.00010-0

[3] Zafar, M.S. (2020). Prosthodontic applications of polymethyl methacrylate (PMMA): An update. Polymers, 12(10): 2299. https://doi.org/10.3390/polym12102299

[4] Wang, X., Xu, S., Xu, W. (2011). Luminescent properties of dye-PMMA composite nanospheres. Physical Chemistry Chemical Physics, 13(4): 1560-1567. https://doi.org/10.1039/c0cp00929f

[5] Jessy, R.S., Ibrahim, M.H. (2014). Biodegradability and biocompatibility of polymers with emphasis on bone scaffolding: a brief review. International Journal of Scientific and Research Publications, 4(7).

[6] Díez-Pascual, A.M. (2022). PMMA-based nanocomposites for odontology applications: A state-of-the-art. International Journal of Molecular Sciences, 23(18): 10288. https://doi.org/10.3390/ijms231810288

[7] Ahamad Said, M.N., Hasbullah, N.A., Rosdi, M.R.H., Musa, M.S., Rusli, A., Ariffin, A., Shafiq, M.D. (2022). Polymerization and applications of poly (methyl methacrylate)-graphene oxide nanocomposites: A review. ACS omega, 7(51): 47490-47503. https://doi.org/10.1021/acsomega.2c04483

[8] Hameed, D.A., Ameer, N.A. (2020). Dental fillers enhanced by nanomaterial's: Oral health-related diagnostic and therapeutic methods. Executive Editor, 11(02): 788.

[9] Radha, G., Balakumar, S., Venkatesan, B., Vellaichamy, E. (2017). A novel nano-hydroxyapatite—PMMA hybrid scaffolds adopted by conjugated thermal induced phase separation (TIPS) and wet-chemical approach: Analysis of its mechanical and biological properties. Materials Science and Engineering: C, 75: 221-228. https://doi.org/10.1016/j.msec.2016.12.133

[10] Partheniadis, I., Papanikolaou, T., Noisternig, M.F., Griesser, U.J., Kantiranis, N., Nikolakakis, I. (2019). Structure reinforcement of porous hydroxyapatite pellets using sodium carbonate as sintering aid: Microstructure, secondary phases and mechanical properties. Advanced Powder Technology, 30(8): 1642-1654. https://doi.org/10.1016/j.apt.2019.05.013

[11] Shashvatt, U., Aris, H., Blaney, L. (2017). Evaluation of animal manure composition for protection of sensitive

water supplies through nutrient recovery processes. In Chemistry and water, pp. 469-509. https://doi.org/10.1016/B978-0-12-809330-6.00013-1

[12] Mazumder, S., Nayak, A.K., Ara, T.J., Hasnain, M.S. (2019). Hydroxyapatite composites for dentistry. Applications of Nanocomposite Materials in Dentistry, 123-143. https://doi.org/10.1016/B978-0-12-813742-0.00007-9

[13] Khoo, W., Nor, F.M., Ardhyananta, H., Kurniawan, D. (2015). Preparation of natural hydroxyapatite from bovine femur bones using calcination at various temperatures. Procedia Manufacturing, 2: 196-201. https://doi.org/10.1016/j.promfg.2015.07.034

[14] Abdullah, N.H., Mohamed Noor, A.A., Mat Rasat, M.S., Mamat, S., Mohamed, M., Mohd Shohaimi, N.A., Ab Halim, A.Z., Shukri, N.M., Abdul Razab, M.K.A., Mohd Amin, M.F. (2020). Preparation and characterization of calcium hydroxyphosphate (hydroxyapatite) from tilapia fish bones and scales via calcination method. In Materials Science Forum, 1010: 596-601. https://doi.org/10.4028/www.scientific.net/MSF.1010.596

[15] Fleischmann, C., Lievenbrück, M., Ritter, H. (2015). Polymers and dyes: Developments and applications. Polymers, 7(4): 717-746. https://doi.org/10.3390/polym7040717

[16] Spence, C. (2023). Saffron: The colourful spice. International Journal of Gastronomy and Food Science, 34: 100821. https://doi.org/10.1016/j.ijgfs.2023.100821

[17] Carmona, M., Zalacain, A., Salinas, M.R., Alonso, G.L. (2007). A new approach to saffron aroma. Critical Reviews in Food Science and Nutrition, 47(2): 145-159. https://doi.org/10.1080/10408390600626511

[18] Naim, N., Bouymajane, A., El Majdoub, Y.O., et al. (2023). Flavonoid composition and antibacterial properties of Crocus sativus L. petal extracts. Molecules, 28(1): 186. https://doi.org/10.3390/molecules28010186

[19] Hammed, D.A., Shinen, M.H., Obayes, A.I. (2024). Extracting a plant dye (Saffran dye) used as antibiotic to treat bacterial diseases. Letters in High Energy Physics, 2024: 524-532. https://lettersinhighenergyphysics.com/index.php/LHEP/article/view/625

[20] Esfahani, M.K., Abedi, M., Bahreini, Z. (2021). The effect of ethanol-water mixture on ultrasonic extraction of crocin from saffron. Saffron Agronomy and Technology, 9(3): 285-293. https://doi.org/10.22048/jsat.2021.49280.1146

[21] Ouyang, J., Huang, H., Chen, X., Chen, J. (2020). Biodegradable Polymer/TiO2 nanotubes loaded roxithromycin as nanoarray capsules for long-lasting antibacterial properties of titanium implant. Journal of Nanomaterials, 2020(1): 5432926. https://doi.org/10.1155/2020/5432926

[22] ten Elshof, J.E. (2015). Chemical solution deposition techniques for epitaxial growth of complex oxides. In Epitaxial Growth of Complex Metal Oxides, pp. 69-93. https://doi.org/10.1016/B978-1-78242-245-7.00004-X

[23] Said, A.M., Zeidan, M.S., Bassuoni, M.T., Tian, Y. (2012). Properties of concrete incorporating nano-silica. Construction and Building Materials, 36: 838-844. https://doi.org/10.1016/j.conbuildmat.2012.06.044

[24] Mondal, S., Mondal, B., Dey, A., Mukhopadhyay, S.S. (2012). Studies on processing and characterization of hydroxyapatite biomaterials from different bio wastes. Journal of Minerals and Materials Characterization and Engineering, 11(1): 55–67. https://doi.org/10.4236/jmmce.2012.111005

[25] Ashwitha, A., Thamizharasan, K., Bhatt, P. (2020). Optimization of hydroxyapatite (HAp) extraction from scales of Sardinella longiceps and its conjugative effect with immunostimulants. SN Applied Sciences, 2: 1-8. https://doi.org/10.1007/s42452-020-3057-9

[26] Chang, S. (2012). Analysis of polymer standards by Fourier transform infrared spectroscopy-attenuated total reflectance and pyrolysis gas chromatography/mass spectroscopy and the creation of searchable libraries. Forensic Science Intership Marshall University Forensic Science Program, pp. 1-46.

[27] An, J., Song, Y., Zhao, J., Xu, B. (2023). Antifungal efficiency and cytocompatibility of polymethyl methacrylate modified with zinc dimethacrylate. Frontiers in Cellular and Infection Microbiology, 13: 1138588. https://doi.org/10.3389/fcimb.2023.1138588

[28] Omar, S., Muhamad, M.S., Te Chuan, L., Hadibarata, T., Teh, Z.C. (2019). A review on lead sources, occurrences, health effects, and treatment using hydroxyapatite (HAp) adsorbent made from fish waste. Water, Air, & Soil Pollution, 230: 1-21. https://doi.org/10.1007/s11270-019-4312-9

[29] Hobson, J. (2012). Socrates. Occupational Medicine, 62(5). https://doi.org/10.1093/occmed/kqs085

[30] Shimanouchi, T. (1973). Tables of molecular vibrational frequencies: Part 6. Journal of Physical and Chemical Reference Data, 2(1): 121-162. https://doi.org/10.1063/1.3253114

[31] Hossain, M.S., Ahmed, S. (2023). FTIR spectrum analysis to predict the crystalline and amorphous phases of hydroxyapatite: a comparison of vibrational motion to reflection. RSC Advances, 13(21): 14625-14630. https://doi.org/10.1039/d3ra02580b

[32] Mohonta, S.K., Maria, K.H., Rahman, S., Das, H., Hoque, S.M. (2021). Synthesis of hydroxyapatite nanoparticle and role of its size in hydroxyapatite/chitosan-gelatin biocomposite for bone grafting. International Nano Letters, 11: 381-393. https://doi.org/10.1007/s40089-021-00347-9

[33] Aldosari, M.A., Darwish, S.S., Adam, M.A., Elmarzugi, N.A., Ahmed, S.M. (2019). Evaluation of preventive performance of kaolin and calcium hydroxide nanocomposites in strengthening the outdoor carved limestone. Archaeological and Anthropological Sciences, 11(7): 3389-3405. https://doi.org/10.1007/s12520-018-0741-4

[34] Pasteur, L. (1964). Organic chemistry I. A History of Chemistry, pp. 749-800. https://doi.org/10.1007/978-1-349-00554-3_24

[35] Riau, A.K., Mondal, D., Setiawan, M., Palaniappan, A., Yam, G.H., Liedberg, B., Venkatraman, S.S., Mehta, J.S. (2016). Functionalization of the polymeric surface with bioceramic nanoparticles via a novel, nonthermal dip coating method. ACS applied materials & interfaces, 8(51): 35565-35577. https://doi.org/10.1021/acsami.6b12371

[36] Bakina, O., Svarovskaya, N., Ivanova, L., Glazkova, E., Rodkevich, N., Evstigneev, V., Evstigneev, M., Mosunov, A., Lerner, M. (2023). New PMMA-based hydroxyapatite/ZnFe2O4/ZnO composite with

antibacterial performance and low toxicity. Biomimetics, 8(6): 488. https://doi.org/10.3390/biomimetics8060488
[37] Ahmed, J.K., Abdulamer, Z.J., Jasim, M., Bahate, M.A. (2017). Effects of natural pigments on the poly (methyl methacrylate) biopolymer. in 16 th Global Annual Oncologists Meeting, p. 5956. https://doi.org/10.4172/1948-5956-C1-096
[38] Laska-Leśniewicz, A., Raczyńska, M., Wrotniak, M., Sobczyk-Guzenda, A. (2019). Changes of structure and properties of PMMA-based bone cements with hydroxyapatite after degradation process. Engineering of Biomaterials, 22(151): 9-16.
[39] Wilson, B.K., Prud'homme, R.K. (2021). Nanoparticle size distribution quantification from transmission electron microscopy (TEM) of ruthenium tetroxide stained polymeric nanoparticles. Journal of Colloid and Interface Science, 604: 208-220. https://doi.org/10.1016/j.jcis.2021.04.081
[40] Zhang, S., Wang, C. (2023). Precise analysis of nanoparticle size distribution in TEM image. Methods and Protocols, 6(4): 63. https://doi.org/10.3390/mps6040063
[41] Yang, B., Li, M., Wu, Y., Huang, J., Zhang, H., Deng, C. (2013). Preparation and characterization of bone-like hydroxyapatite/poly (methyl methacrylate) composite biomaterials. Science and Engineering of Composite Materials, 20(2): 147-153. https://doi.org/10.1515/secm-2012-0079
[42] Hussein, A.K. (2014). Effects of hydroxyapatite on some mechanical properties on dental filling materials. University of Babylon. https://doi.org/10.5005/jp/books/13101_7
[43] Kusdianto, K., Widiyastuti, W., Shimada, M., Qomariyah, L., Winardi, S. (2020). Fabrication of ZnO-SiO2 nanocomposite materials prepared by a spray pyrolysis for the photocatalytic activity under UV and sunlight irradiations. In IOP Conference Series: Materials Science and Engineering, 778(1): 012105. https://doi.org/10.1088/1757-899X/778/1/012105
[44] Thiab, S.S., Mohammad, Q.A.K., Mahdi, A.G. (2010). The effect of shade and curing time on depth of cure (DOC) in two types of composites, polymerized with a halogen light cure system. Kufa Medical Journal, 13(1): 168-185.
[45] Mohaimeed, A.A., Hameed, D.A. (2020). Some of mechanical properties to nanosilica and nanographene used in medical application. TEST Engineering & Management, 2008: 2008-2015.
[46] Kokkinaki, F., Ordoudi, S.A. (2023). Insights into the FTIR spectral fingerprint of saffron (Crocus sativus L.) stigmas after gentle drying treatments. Food and Bioprocess Technology, 16(12): 3057-3072. https://doi.org/10.1007/s11947-023-03119-9
[47] Sarfarazi, M., Jafari, S.M., Rajabzadeh, G., Feizi, J. (2019). Development of an environmentally-friendly solvent-free extraction of saffron bioactives using subcritical water. LWT, 114: 108428. https://doi.org/10.1016/j.lwt.2019.108428
[48] Jiao, Y., Okada, M., Nutan, B., et al. (2023). Fabrication of a fish-bone-inspired inorganic–organic composite membrane. Polymers, 15(20): 4190. https://doi.org/10.3390/polym15204190
[49] Munir, M.U., Salman, S., Ihsan, A., Elsaman, T. (2022). Synthesis, characterization, functionalization and bio-applications of hydroxyapatite nanomaterials: An overview. International Journal of Nanomedicine, 17: 1903-1925.
[50] D'Archivio, A.A., Di Donato, F., Foschi, M., Maggi, M.A., Ruggieri, F. (2018). UHPLC analysis of saffron (Crocus sativus L.): optimization of separation using chemometrics and detection of minor crocetin esters. Molecules, 23(8): 1851. https://doi.org/10.3390/molecules23081851
[51] Melnyk, J.P., Wang, S., Marcone, M.F. (2010). Chemical and biological properties of the world's most expensive spice: Saffron. Food Research International, 43(8): 1981-1989. https://doi.org/10.1016/j.foodres.2010.07.033
[52] Licón, C., Carmona, M., Llorens, S., Berruga, M.I., Alonso, G.L. (2010). Potential healthy effects of saffron spice (Crocus sativus L. stigmas) consumption. Funct Plant Sci Biotechnol, 4(2): 64-73.
[53] Pintado, C., de Miguel, A., Acevedo, O., Nozal, L., Novella, J.L., Rotger, R. (2011). Bactericidal effect of saffron (Crocus sativus L.) on Salmonella enterica during storage. Food Control, 22(3-4): 638-642. https://doi.org/10.1016/j.foodcont.2010.09.031
[54] Riaz, U., Ashraf, S.M. (2014). Charecterization of polymer blends using FTIR spectroscopy. Charecterization Polym. Blends, pp. 625–678. https://doi.org/10.1416/j.jtumed.2014.11.001
[55] Saskianti, T., Wardhani, K.K., Fadhila, N., Wahluyo, S., Dewi, A.M., Nugraha, A.P., Ernawati, D.S., Kanawa, M. (2024). Polymethylmethacrylate-hydroxyapatite antibacterial and antifungal activity against oral bacteria: An in vitro study. Journal of Taibah University Medical Sciences, 19(1): 190-197. https://doi.org/10.1016/j.jtumed.2023.11.001
[56] Akraa, M., Hasan, A.S., Kadhim, M.J.H. (2020). Spectroscopy characterization of ethylene vinyl acetate degradation by different kinds of accelerated aging. Baghdad Science Journal, 17(3): 0795-0795. https://doi.org/10.21123/bsj.2020.17.3.0795